Scattering of acoustic waves in air and water filled 3D stereo-lithographical (STL) porous rigid materials

Haydar Aygun, PhD

London South Bank University

School of the Built Environment and Architecture, 103 Borough Rd, London, SE1 0AA, UK

ABSTRACT

The scattering of acoustic waves propagating in porous rigid 3D stereolithographical materials that are made of resin, has been investigated. 3D stereolithographical (STL) materials were obtained using a form of rapid prototyping that allows complex solid objects to be manufactured directly from 3D computer models in the form of successive layers of light-cured resin. Relative variation of velocity and attenuation of 3D materials in air filled and water filled media has been predicted at normal and oblique directions. The scattering perturbation is similar to diffusion waves at low frequency while dispersion velocity and attenuation change with respect to square root of angular frequency and with respect to angular frequency at high frequency respectively.

1. INTRODUCTION

Poroelastic materials may be employed for noise control in aircraft, buildings and various other engineering applications. According to Rayleigh [1], 'the fundamental characteristic of porous materials treated to reduce noise is that the produced fluid flow through the poroelastic material is opposed because of the frictional force produced by the fibres or the cell walls on the fluid. This mechanism allows the energy to be absorbed from the acoustic wave and to be converted into heat.' The most widely-exploited and acknowledged absorption mechanism in porous materials is viscous friction due to relative motion between solid and fluid. If the frame of the porous material is viscoelastic then other dissipative mechanisms are possible.

Biot theory has been used extensively to describe the wave propagation in rigid porous media, specifically developed to describe acoustic wave propagation in fluid-saturated porous elastic media [2, 3]. Biot theory predicts two compressional waves (fast and slow waves), when the waves propagating through the solid frame and fluid are in-phase and out-of-phase respectively, and a shear wave. It allows for an arbitrary microstructure, with separate motions considered for the solid elastic framework and the interspersed fluid, induced by the acoustic wave, and also includes energy loss due to viscous friction between solid and fluid. The anisotropic pore structure and elasticity of cancellous bone cause wave speeds and attenuation in cancellous bone to vary with angle [4].

Previous work on the influence of anisotropic pore structure and elasticity in cancellous bone has been extended by developing an anisotropic Biot-Allard model allowing for angle-dependent

elasticity, and angle-and-porosity dependent tortuosity [4]. The extreme angle dependence of tortuosity corresponding to the parallel plate microstructure has been replaced by angle-and-porosity dependent tortuosity values based on data for slow wave transmission through air-filled stereolithography (STL) replicas [5]. It has been suggested that the anisotropic Biot-Allard model could be used to give further insight into the factors that have the most important influence on the angle dependency of wave speeds and attenuation in porous rigid materials. Nevertheless the applicability of Biot-based theories to ultrasonic propagation in porous rigid medium remains in question given the expected role of scattering which is neglected in these theories. Aygün *et al.* [6, 7, 8] have transmitted ultrasonic signals through water saturated stereolithograpical replica samples in the form of 57 mm cubes with microstructural dimensions that are 13 times real scale at normal angle and oblique angles. Remarkably, it is found that the expected occurrence of scattering does not cause significant discrepancies between predictions and data at 100 kHz, perhaps as a consequence of the fact that the samples behave as low pass filters.

Boutin [9] has investigated low frequency scattering of acoustic waves propagation through heterogeneous media made of air and motionless inclusions. The method developed by Boutin has been used to investigate relative variation of velocity and attenuation of 3D materials in air filled and water filled media at normal and oblique incidences.

2. STEREO-LITHOGRAPHY MANUFACTURING SYSTEM

Stereo-lithography (STL) is a form of rapid prototyping that allows complex solid objects to be manufactured directly from 3D computer models in the form of successive layers of light-cured resin [10]. There are two stages to stereolithography, design and manufacturing. During the design stage the required object is initially created using standard 3D solid modelling techniques and then converted into the stereolithography format consisting of a series of thin slices. The stereolithography manufacturing system consists of a vat of light-sensitive resin with an elevator and computer-controlled scanning laser. At the start of the process, the elevator is positioned just below the surface (typically 0.1 mm) of the liquid stereolithography resin. The laser scanner "prints" the bottom layer onto the resin surface, which solidifies upon exposure to the laser beam. The elevator then moves down by an incremental distance and the stereolithography resin is respread over the surface of the vat prior to the next scan. As successive solid layers are formed, they bond to produce a single solid object. When the model is completed the elevator is raised and the unused resin is allowed to drain. The laser cures the stereolithography resin to approximately 60%. The curing process is completed in an ultraviolet oven. The resolution of the stereolithography process is governed by the laser spot

size and the vertical movement of the elevator. Typically, the laser spot diameter will be better than 0.3 mm and the elevator movement resolution will be about 2.5μm.

The primary reason for creating stereolithography samples is that multiple copies may be created. This is particularly valuable for mechanical testing, where measurement in one direction may damage a sample and preclude testing in other orthogonal directions. The models were created at a magnification of x13 to ensure spatial fidelity between the voxel size of the microCT scan of the original natural samples and the minimum wall thickness achievable with STL. Material 'corrosion' due to degradation can be simulated physically by corresponding stereolithographical samples.
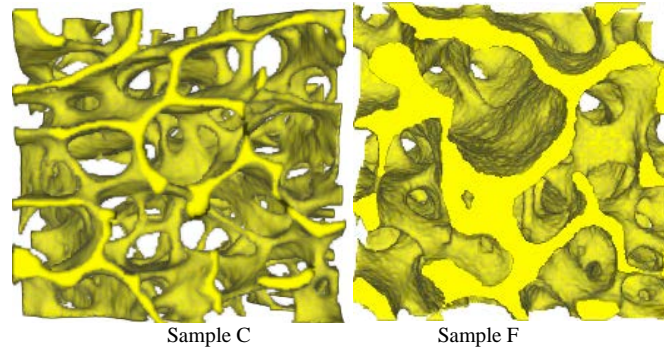

Sample C   Sample F

Figure 1: views of 3D stereolithographical samples.

3. SCATTERING OF PLANE WAVES

The effects of scattering on plane wave propagation in porous medium has been investigated using a model developed by Boutin [9] to determine wave velocity and attenuation in rigid porous materials.

A harmonic plane wave propagating in a given direction of unit vector d is given by

$$P = P_0 e^{-(iH_d x.d + i\omega t)} \tag{1}$$

where P_0 is the amplitude of zeroth order pressure, H_d is the complex wave number, ω is the angular frequency, d is the unit vector, t is the time taken, and x is the distance travelled.

The wave velocity C_d, wavelength λ_d, and attenuation ξ_d in the propagation direction are related to the wave number by [9]

$$H_d = \frac{\omega}{C_d}(1 - i\xi_d) \tag{2}$$

where $C_d = \frac{\omega}{H_r}$, $\lambda_d = \frac{2\pi}{H_r}$, $\xi_d = -\frac{H_i}{H_r}$, H_i is the imaginary part of complex wave number and H_r is the real part of complex wave number.

Harmonic plane wave shows a strong dispersion due to changes in frequency dependent dynamic permeability leading to that;

a) A diffusion wave at low frequency, $\omega < \omega_d$, produces $C_d \approx \sqrt{\frac{\omega}{\omega_c}} \sqrt{\frac{P_e}{\rho^e \alpha_\infty}}$ and $\xi_d \approx 1 - O\sqrt{\frac{\omega}{\omega_c}}$.

b) A propagation wave at high frequency, $\omega > \omega_d$, produces $C_d \approx \sqrt{\frac{\gamma P_e}{\rho^e \alpha_\infty}}$ and $\xi_d \approx \sqrt{\frac{\omega_c}{\omega}}$.

where ρ^e is the density of water, α_∞ is the tortuosity, ω is the angular frequency, ω_d is the diffraction frequency, ω_c is the critical frequency, P_e is the equilibrium state pressure, γ is the specific heat ratio. The macro-pressure can be expressed as [9]

$$P_m = P_0(e^{-i\widetilde{H_d}x.d} + O(\epsilon^3)) \tag{3}$$

where $\widetilde{H_d} = H_d - H_d Q_d(-iH_d)^2$ and $O(\epsilon^3)$ is the correction order given by $O\left(\frac{l^3}{(\lambda/2\pi)^3}\right)$.

Consequently the wave number is modified by diffraction yielding that [9];

$$\widetilde{H_d} = \frac{\omega}{C_d}(1 - i\xi_d)\left[1 + |Q_d|(\cos\chi + \sin\chi)x\left(\frac{\omega(1-i\xi_d)}{C_d}\right)^2\right] \tag{4}$$

Apparent wave velocity can be derived as follow;

$$\widetilde{C_d} = C_d\left[1 - |Q_d|\left(\frac{\omega}{C_d}\right)^2((1-\xi_d^2)(\cos\chi + \xi_d\sin\chi) + 2\xi_d(\cos\chi - \xi_d\sin\chi)\right] \tag{5}$$

Apparent attenuation factor can be derived as follow;

$$\widetilde{\xi_d} = \xi_d + |Q_d|\left(\frac{\omega}{C_d}\right)^2(2\xi_d(1+\xi_d^2)\cos\chi - \sin\chi + \xi_d^4\sin\chi) \tag{6}$$

Apparent wave velocity and attenuation explain the differences between the effects of scattering on poroacoustic waves and on thermo-elastic waves.

Frequency dependent wave velocity and attenuation in viscous regime are given by equations below respectively [9];

$$\widetilde{C_d} = C_d\left[1 + 2Q_{d0}\left(\frac{\omega}{C_d}\right)^2\right] \tag{7}$$

$$\widetilde{\xi_d} = \xi_d + 4Q_{d0}\left(\frac{\omega}{C_d}\right)^2 \tag{8}$$

where ξ_d is the attenuation, C_d is the wave number, and Q_{d0} is the frequency dependent complex coefficient.

In the inertial regime, the waves will be damped while they propagate through porous rigid media. Wave velocity and attenuation are given by following equations [9];

$$\widetilde{C_d} = C_d\left[1 - 2Q_{d0}\left(\frac{\omega}{C_d}\right)^2(\cos\chi + 3\xi_d\sin\chi)\right] \tag{9}$$

$$\widetilde{\xi_d} = \xi_d - |Q_d|\left(\frac{\omega}{C_d}\right)^2[\sin\chi - 2\xi_d\cos\chi] \tag{10}$$

where Q_d is the frequency dependent complex coefficient and χ is the angle of incidence.

Critical frequency for porous rigid materials is given by:

$$\omega_c = \frac{\phi\mu}{\kappa\rho^e\alpha_\infty} \tag{11}$$

where ϕ is the porosity, ρ^e is the density of water, 1000 kg/m^3, α_∞ is the tortuosity, K is the permeability, and μ is the gas viscosity.

4. RESULTS

Frequency dependent relative variation of wave velocity and attenuation are predicted in viscoinertia regime at 1 MHz and in inertia regime at 1 kHz for both oblique and normal incidences in air and water filled medium. The results of diffraction effects within the viscoinertial regime are shown in Figures 2, 3 and 4. Anisotropic effect can be seen throughout frequency range. In Figure 2a, velocity variation reduces in both direction while attenuation significantly increases in both direction and oblique velocity becomes more attenuated. The variations in air filled medium shown Figure 2b are about 35 times higher than the variations in water filled medium. Diffraction effect on the relative variation of wave velocity and attenuation in inertial regime are shown in Figure 3. Relative variation of attenuation increases throughout frequency range at normal and oblique directions in water filled medium. This means that attenuation is not affected by diffraction in this regime. Wave velocity increases in normal direction while it is effected by diffraction and decreases at oblique direction.

Wave velocity and attenuation for sample F at normal and oblique direction in water and air filled medium are shown in Figure 4. Relative velocity at oblique incidence is decreased by diffraction while others are not affected by diffraction in water filled porous rigid medium.
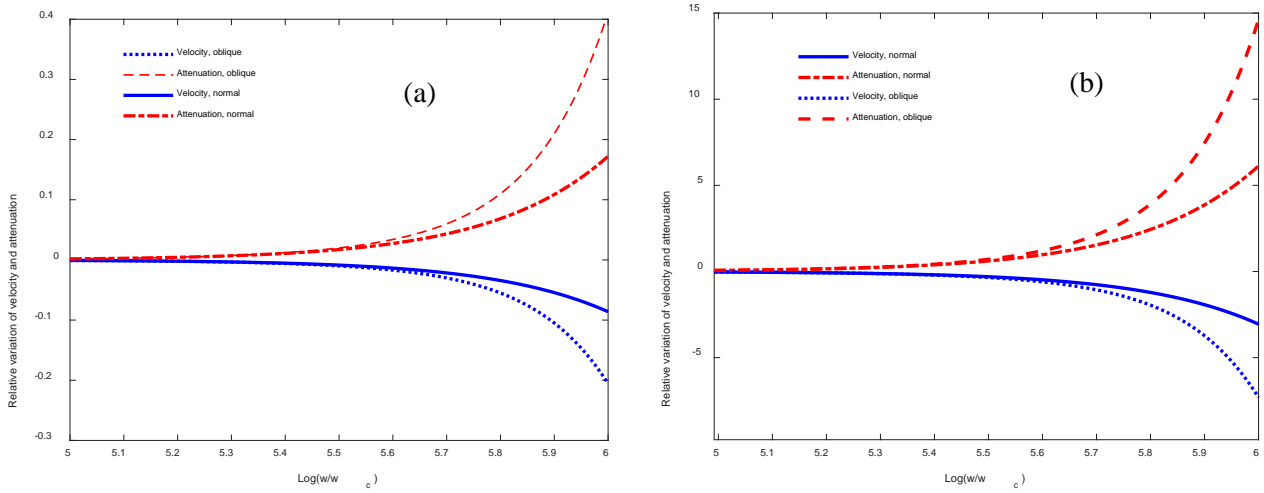

Figure 2: Relative variation of velocity $\left(\frac{\widetilde{C_d}-C}{C}\right)$ and variation of attenuation $(\widetilde{\xi_d} - \xi_d)$ versus frequency ratio in viscoinertial regime at 1 MHz; a) water filled STL sample C and b) air filled STL sample C.
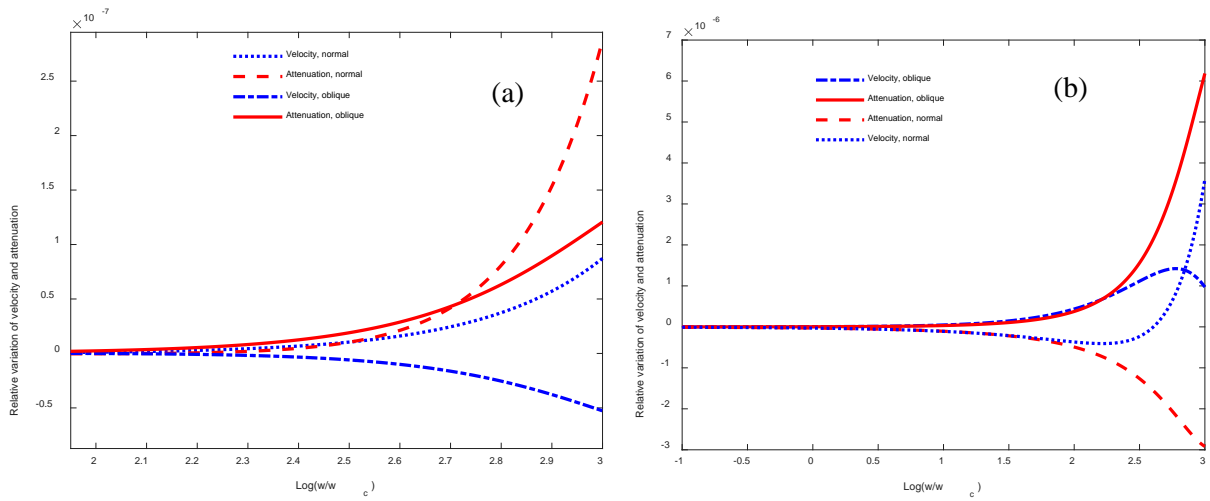

Figure 3: Relative variation of velocity $\left(\frac{\widetilde{C_d}-C}{C}\right)$ and variation of attenuation $(\widetilde{\xi_d} - \xi_d)$ versus frequency ratio in inertial regime at 1 kHz; a) water filled STL sample C and b) air filled STL sample C.
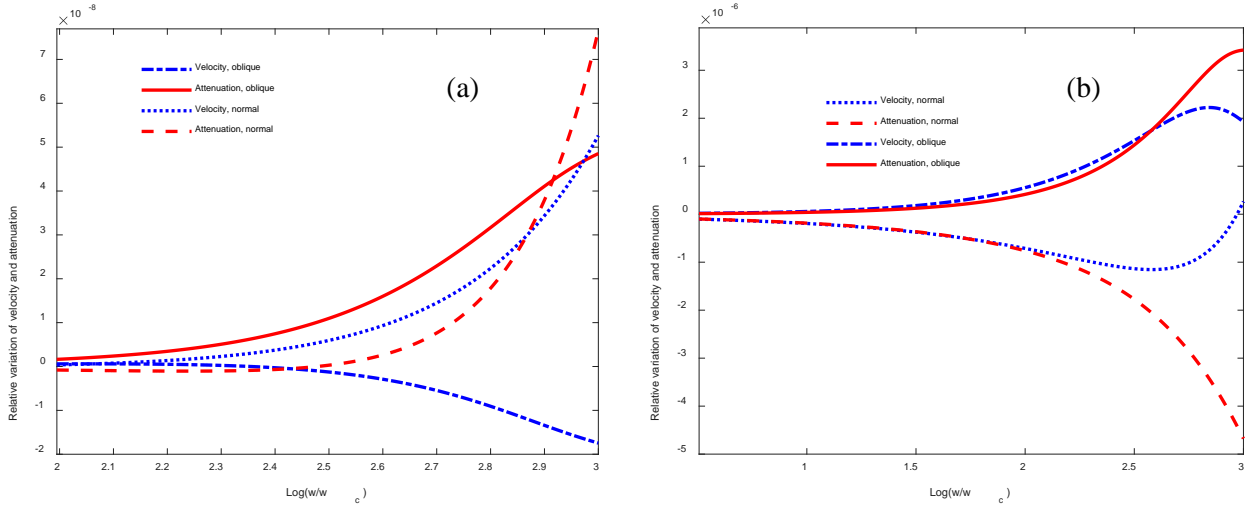
Figure 4: Relative variation of velocity $\left(\frac{\widetilde{C_d}-C}{C}\right)$ and attenuation $(\widetilde{\xi_d} - \xi_d)$ versus frequency ratio in inertia regime at 1 kHz; a) water filled STL sample F and b) air filled STL sample F.

5. CONCLUSION

A scattering model developed by Boutin has been applied to 3D STL porous rigid materials to determine the relative variation of velocity and attenuation at normal and oblique incidences. The results in air filled medium has been compared with the ones in water filled medium. In water filled medium, mostly wave velocity is effected by diffraction at oblique direction while in air filled medium, wave is attenuated at normal direction for both studied samples. The anisotropic pore structure and elasticity of STL samples cause wave speed and attenuation in rigid porous samples to vary with angle.

6. ACKNOWLEDGEMENTS

7. REFERENCES

1. Lord Rayleigh, *"Theory of Sound"* (London, 1926) Vol.(I), and (Dover, New York, 1945), Vol.(II).
2. Biot M. A., 1956 Theory of propagation of elastic waves in a fluid saturated porous solid, I. Low frequency range. *J. Acoust. Soc. Am.* **28** 168–1178.
3. Biot M. A., 1956 Theory of propagation of elastic waves in a fluid saturated porous solid, II. High frequency range. *J. Acoust. Soc. Am.* **28** 179–191.
4. Aygün H., Attenborough K., Postema M., Lauriks W., and Langton C. M., 2009, Predictions of angle dependent tortuosity and elasticity effects on sound propagation in cancellous bone. *J. Acoust. Soc. Am.* 126 (6), 3286-3290.
5. Attenborough K., Qin Q., Fagan M. J., Shin H.-C., and Langton C. M., 2005 Measurements of tortuosity in stereolithographical bone replicas using audio-frequency pulses. *J. Acous. Soc Am.* **118** 2779-2782.
6. Aygün H., Attenborough K., Lauriks W., and Langton C. M., 2010, "Ultrasonic wave propagation in Stereo-lithographical bone replicas." *J. Acoust. Soc. Am.* 127 (6), 3781 – 3789.

7. Aygün H., Attenborough K., Lauriks W., Rubini P.A., and Langton C. M., 2011, "Wave propagation in stereo-lithographical (STL) bone replicas at oblique incidence." *Applied Acoustics*. 72 (7) 458 – 463.

8. Aygün H. and Barlow C. 2014, "Behaviour of ultrasonic waves in porous rigid materials: anisotropic Biot-Attenborough model." *Anglo-French Physical Acoustic Conference*, 15 – 17 January 2014, Surrey, UK.

9. Boutin, C. 2007. "Rayleigh scattering of acoustic waves in rigid porous media". *J. Acoust. Soc. Am.* Volume (122), 1888.

10. Langton C M, Whitehead M A, Langton D K, and Langley G, 1997. Development of a cancellous bone structural model by stereolithography for ultrasound characterisation of the calcaneus. *Med. Eng. Phys.* **19** 599-604.